Government of Western Australia

Department of **Mines, Industry Regulation and Safety**

REPORT 187

DETECTION AND IDENTIFICATION OF RARE EARTH ELEMENTS USING HYPERSPECTRAL TECHNIQUES

by S Morin-Ka

Geological Survey of Western Australia

Government of **Western Australia**
Department of **Mines, Industry Regulation and Safety**

REPORT 187

DETECTION AND IDENTIFICATION OF RARE EARTH ELEMENTS USING HYPERSPECTRAL TECHNIQUES

by

S Morin-Ka

PERTH 2018

Geological Survey of Western Australia

MINISTER FOR MINES AND PETROLEUM
Hon Bill Johnston MLA

DIRECTOR GENERAL, DEPARTMENT OF MINES, INDUSTRY REGULATION AND SAFETY
David Smith

EXECUTIVE DIRECTOR, GEOSCIENCE AND RESOURCE STRATEGY
Jeff Haworth

REFERENCE
The recommended reference for this publication is:
Morin-Ka, S 2018, Detection and distinction of rare earth elements using hyperspectral technologies: Geological Survey of Western Australia, Report 187, 16p.

ISBN 978-1-74168-819-1

A catalogue record for this book is available from the National Library of Australia

Grid references in this publication refer to the Geocentric Datum of Australia 1994 (GDA94). Locations mentioned in the text are referenced using latitude and longitude.

Published 2018 by the Geological Survey of Western Australia
This Report is published in digital format (PDF) and is available online at <www.dmp.wa.gov.au/GSWApublications>.

Further details of geological publications and maps produced by the Geological Survey of Western Australia are available from:
Information Centre
Department of Mines, Industry Regulation and Safety
100 Plain Street
EAST PERTH WESTERN AUSTRALIA 6004
Telephone: +61 8 9222 3459 Facsimile: +61 8 9222 3444
www.dmp.wa.gov.au/GSWApublications

Cover photograph: John Galt rare earth element prospect in the east Kimberley region, Western Australia

Contents

Figures

Tables

Detection and identification of rare earth elements using hyperspectral techniques

by

S Morin-Ka

Abstract

The HyLogger was used to collect hyperspectral data, in visible and near-infrared (VNIR), short-wave infrared (SWIR) and thermal infrared (TIR) spectral ranges, for 15 rare earth oxides (REO) powder standards with >99.99% purity. Each REO returned a unique spectral signature exhibiting repeatable, consistent and sharp absorption features in the VNIR and SWIR ranges, but no detectable features in the TIR range. The three most prominent absorption features from light REO (at 747, 804 and 872 nm) and heavy REO (at 656, 804 and 908 nm) were selected to create spectral algorithms, or 'scalars', to automatically identify rare earth elements (REE) in any VNIR spectrum. These scalars were tested against several naturally occurring examples of REE, including: selected specimens of common REE-bearing minerals; more continuous drillcores from the carbonatite-hosted, light rare earth elements (LREE)-dominant Mount Weld and Cummins Range deposits; and outcrop samples from the hydrothermal vein-hosted, heavy rare earth elements (HREE)-dominant Browns Range deposit. Diagnostic LREE or HREE signatures were detected by the scalars in all these examples, with their distribution confirmed by comparison with independently acquired REE chemical data and petrological identification. However, REE signatures can be subdued by broad overlapping Fe^{3+} absorption in the VNIR range. This study demonstrates that reflectance spectroscopy is a viable exploration tool for rapid, non-destructive detection and broad characterization of REE mineralization in powders, rock chips, drillcore, or outcrop.

KEYWORDS: hyperspectral, HyLogger, rare earth elements, rare earth oxides, spectrometry

Introduction

Rare earth elements (REE) can be divided into light rare earth elements (LREE) and heavy rare earth elements (HREE) based on a comparison of their atomic radii and charge. In nature, REE deposits tend to be enriched either in LREE or HREE, with HREE being rarer than LREE. REE and REE-bearing minerals can be detected and their abundance estimated by several methods that include X-ray fluorescence (XRF), X-ray diffraction (XRD) and bulk geochemical analysis. However, these conventional techniques have the limitation that they are destructive, costly or lack portability. Portable-XRF has the added inadequacy that it reports some REE with low accuracies and cannot detect all REE. Studies have demonstrated that REE have specific absorption features in the visible near-infrared (VNIR) spectral range due to energy transitions by 4f-orbital electrons within the REE atoms (Adams, 1965; Turner et al., 2014, 2016). These features are identifiable by hyperspectral technologies with the advantage that they are non-destructive, rapid, transportable and economical (Morin-Ka et al., 2014). The present study examines if a) individual REE can be identified using hyperspectral technologies; b) LREE can be distinguished from HREE in minerals; or c) REE can be accurately detected by the automated or manual interrogation of spectra for REE-enriched materials using The Spectral Geologist (TSG) software. This Report initially provides relevant background information about REE, absorption spectroscopy and the HyLogging system operated by the Department of Mines, Industry Regulation and Safety (DMIRS). The three main study aims are then sequentially addressed, before comments are made about possible limitations and conclusions of the study.

Rare earth elements — chemistry and mineralogy

Rare earth elements are a group of 15 elements with $6s^24f^n$ electronic structure that form stable 3+ ions of similar size and are collectively named the lanthanides plus yttrium (Fig. 1). Minor differences in the geochemical behaviour of individual REE exist due to variations in their atomic number and ionic radii. In addition, cerium can also occur in a 4+ oxidation state and europium can exist in a 2+ oxidation state. Although yttrium has a comparatively low atomic number of 39 compared with most REE, it displays a 3+ ionic charge and has a similar ionic radius (1.019 angstrom [Å]) to holmium (1.015 Å); thus, yttrium is commonly grouped with HREE (Verplanck and Van Gosen, 2011). Compared with HREE, LREE tend to occupy a larger lattice with 8–10 coordination number sites, and are concentrated in carbonates and phosphates. HREE and Y occupy 6–8 coordination number sites and are abundant in oxides and some phosphates (Dill, 2010).

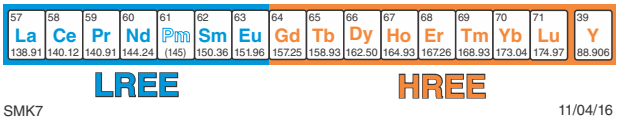

Figure 1. Classification of rare earth elements (REE): light rare earth elements (LREE) in blue and heavy rare earth elements (HREE) in orange

Rare earth elements do not occur as free metals in the Earth's crust, but are contained in naturally occurring minerals consisting of mixtures of various REE and non-metals. Bastnäsite [(Ce,La)(CO_3)F], monazite [(Ce,La,Nd,Th) PO_4], and xenotime [YPO_4] are the three most economically significant minerals of the more than 200 minerals known to contain REE (Christie et al., 1998). Bastnäsite and monazite are the principal sources of LREE, accounting for about 95% of REE used (US Geological Survey, 2018). Xenotime is the principal source for HREE.

Reflectance spectroscopy

Two general processes cause absorption spectral features, electronic (such as crystal field effects and charge transfer), and vibrational processes (such as symmetric/asymmetric stretches and bendings) (Clark, 1999). In addition, crystal field interactions include variables such as ligand type, coordination number and polyhedron asymmetry, which all play a role in the location and intensity of an absorption feature (Görller-Walrand and Binnemans, 1998). Reflectance spectroscopy produces spectra as shown in Figure 2, exhibiting 'features' and forming 'signatures'. Here a feature is defined as an absorption peak corresponding to a wavelength, whereas a signature comprises several features associated with an element or mineral (Fig. 2).

HyLogging system

The HyLogging system comprises the HyLogger and TSG software. The HyLogger 3 (Hancock and Huntington, 2010) is used to acquire spectra. The HyLogger detects VNIR (380–1000 nm), SWIR (1000–2500 nm) and TIR (6000–14 000 nm) wavelength ranges of electromagnetic spectra. The system also captures high-definition RGB images of the scanned sample and the collected spectra are spatially matched with the corresponding RGB image.

Collected spectra are processed using TSG version 7. This program employs a mineral identifier tool called The Spectral Assistant (TSA) that automatically interprets the spectra collected for each 8 mm interval of scanned drillcore. TSA searches for the best match between the stored mineral database and the collected spectra automatically. For each spectrum, TSA provides results for up to two minerals in the VNIR and SWIR ranges, and up to three minerals in the TIR range. Algorithms known as 'scalars' are used to perform calculations to detect specific features in the collected spectra. Mixtures of minerals are often more difficult to interpret than pure minerals using TSA. Downsampling is a processing technique available in TSG that is used to combine several spectra into one spectrum. The combined spectrum displays all the features of the original spectra.

Hyperspectral experiments

This study: a) tests the hyperspectral responses of REE; b) determines if REE can be detected in unprocessed samples, such as hand specimens or core material; c) investigates if LREE or HREE can be differentiated; and d) proposes a new method for automatically detecting and differentiating REE in acquired hyperspectral datasets. The three aims were evaluated in three related experiments, which are documented below.

Rare earth oxides

This section focuses on the detectability of REE with hyperspectral technologies using pure rare earth oxides (REO) as reference materials. In this work, all rare earth elements were tested separately to obtain their unmixed spectral signature.

Methodology

Forty samples of REO reference materials were examined, representing the full suite of the lanthanides and yttrium. Two different REO reference mixtures are used for every element for the purpose of testing possible variations in spectra between samples. The reference sets included mostly oxides, but also included sulphate, phosphate, chloride and carbonate compounds. REO are in micrometric powder form; however, the lanthanum chloride (LaCl) and lanthanum phosphate ($LaPO_4$) are powders with a millimetric grain size. The two sets of REO powders provided by Huntington Hyperspectral Pty Ltd and CSIRO are at least 99.99% pure, with the exception of praseodymium-carbonate-otcahydrate at 99.9% purity and lanthanum-chloride at 32% purity. Glass petri dishes are used as containers to protect the REO from possible external contamination while being scanned. The glass containers have the advantage that they do not produce spectral interference in the VNIR and SWIR ranges. However, the silica in the glass can be detected by the TIR spectrometer. To prevent this, the surface of the petri dish is covered by a REO powder at least one millimetre-thick. Each REO is measured 100 times to produce a single representative spectrum in the VNIR, SWIR and TIR ranges. To achieve this, the HyLogger is configured to a single-spot analysis mode, where a single location is measured the number of desired times and the returned data averaged into a single spectrum.

Results

All REO have a unique spectral signature within the VNIR and SWIR ranges (Fig. 4). In contrast, no unique signatures are observed in the TIR range (Fig. 5). These documented spectral signatures are consistently reproduced between corresponding sets of reference sample powders. Most distinguishing spectral features in the VNIR and SWIR ranges are located between the 400 nm and 1600 nm wavelengths, with neodymium (Nd), samarium (Sm), holmium (Ho), erbium (Er) and thulium (Tm) having the most discernible features.

The TIR range presents broad absorption troughs centred on 6570 and 7145 nm. However, these absorption troughs

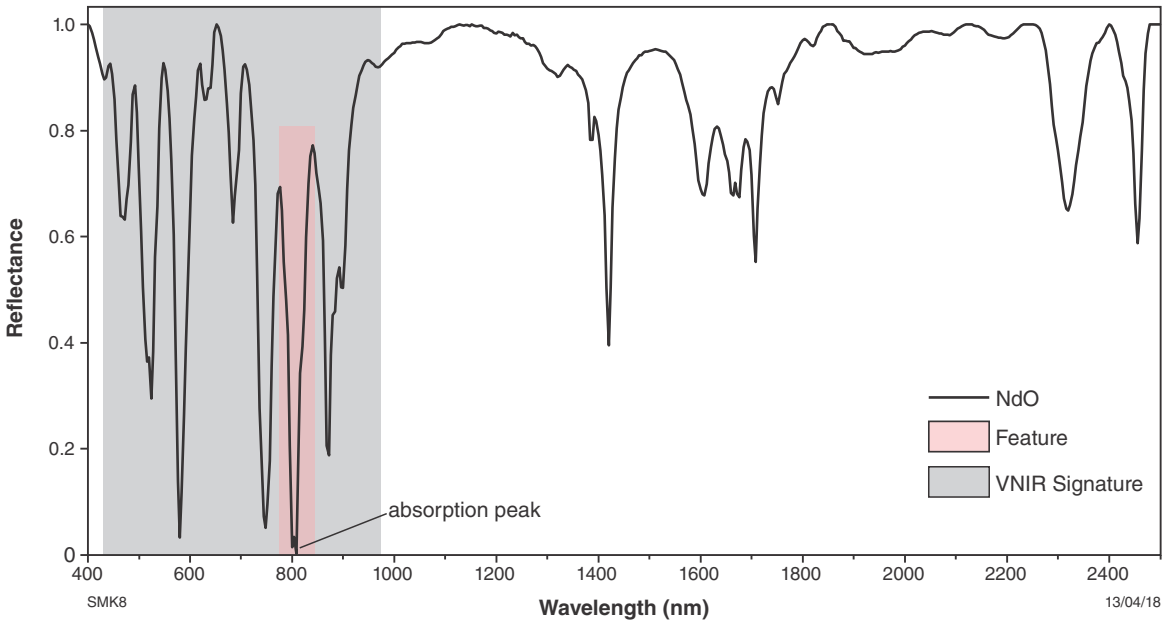

Figure 2. Terminology used to describe spectra using NdO spectrum as an example; a feature is a single absorption peak, while a signature is a combination of several features

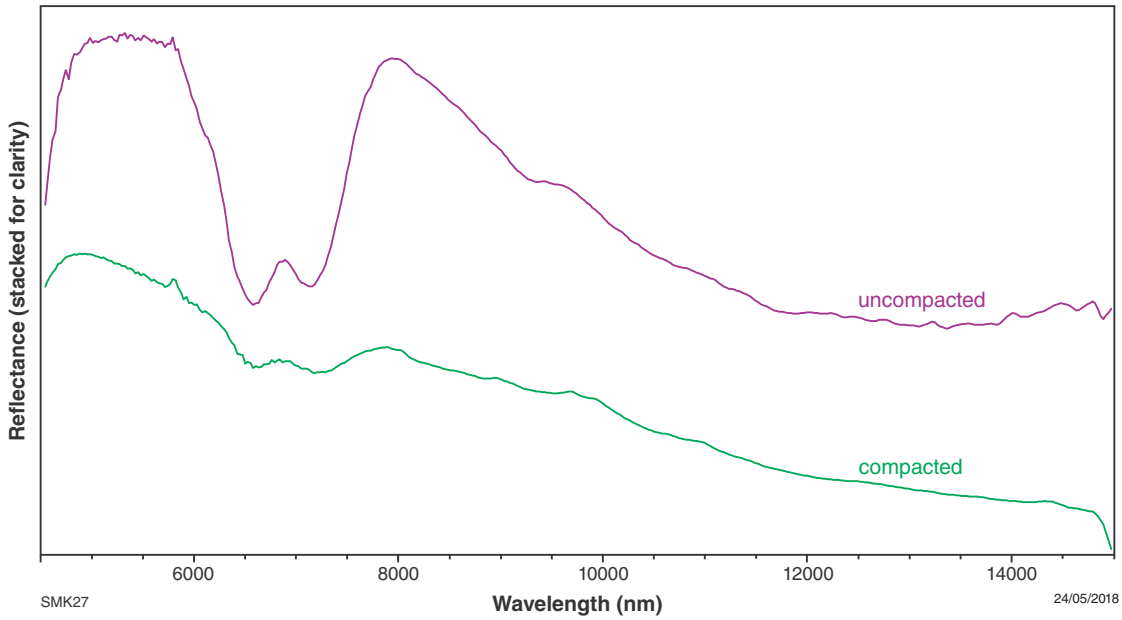

Figure 3. YbO TIR spectra when uncompacted (top spectrum) and compacted (bottom spectrum)

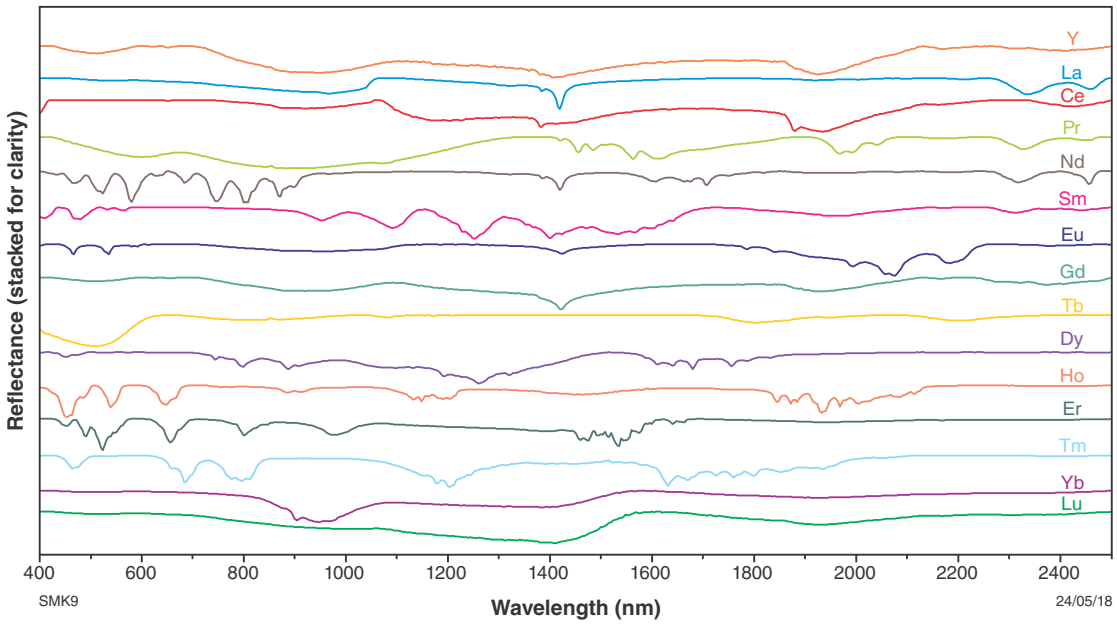

Figure 4. Spectra of rare earth oxides in VNIR and SWIR ranges

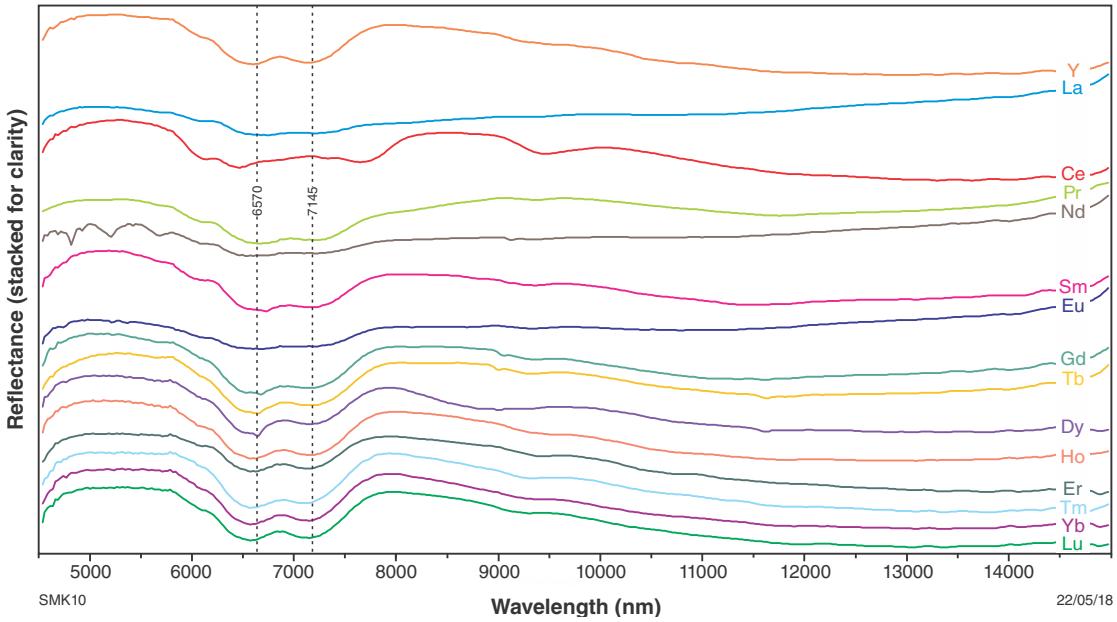

Figure 5. Spectra of rare earth oxides in TIR range

disappear when the samples are rescanned after compaction with a hand mortar. The compacted samples show a reduction in depth of the absorption features as shown in Figure 3. This phenomenon is interpreted as surface scattering of light through the greater volume of finely sized particles of the uncompacted powders, as described in more detail by Hancock et al. (2013). The VNIR/SWIR spectra of the compacted samples remain consistent during repeated testing with the HyLogger. In conclusion, the TIR do not present observable REE signatures that are useful for REE discrimination.

Downsampling

Downsampling is a processing technique available in TSG that is used to combine several spectra into one spectrum. The resulting spectrum conveniently displays all the features of the original spectra. Because most natural mineral occurrences contain REO as mixtures of LREE or HREE, the downsampling technique is applied to the REO spectra to produce a single spectrum for all LREO (Fig. 6) and a single spectrum for all HREO (Fig. 7) in the VNIR and SWIR ranges. Both downsampled spectra exhibit sharp distinctive features forming unique signatures for LREO and HREO. In addition, LREO and HREO signatures display similar features at around 525, 685 and 804 nm wavelengths, thus providing useful information for identifying the presence of any REO.

The downsampled LREO and HREO spectra are then compared with spectral data obtained for common REE minerals, such as apatite, bastnäsite, monazite and parisite, with data sourced from Morin-Ka (2012; Fig. 8; Table 1). The downsampled LREO and REE minerals spectra display strong correlations at about 580, 747, 804 and 872 nm, with weaker correlations at 525 and 685 nm. In contrast, the downsampled HREO spectrum shows close correlation with only the HREE-rich xenotime, with strong absorptions at 648–668, 800–816 and 900–916 nm and weaker correlations at 457, 525 and 540 nm. The LREO and LREE-minerals show correlated features within the range of the spectral spatial resolution of 5 nm, whereas HREO and xenotime show correlated features that are separated by up to 8 nm (Fig. 8).

Rare earth compounds

Praseodymium (Pr) and lanthanum (La) are tested to compare the reflectance spectra associated with their typical compounds. Firstly, a comparison is made between praseodymium oxide (PrO) and praseodymium-carbonate-otcahydrate ($C_3O_9Pr_2{\cdot}8H_2O$). The results demonstrate that PrO shows no REE features in the VNIR range, whereas $C_3O_9Pr_2{\cdot}8H_2O$ displays diagnostic LREE features at 580, 747, 804 and 872 nm (Fig. 9). The second test involved the comparison between lanthanum oxide (LaO), lanthanum orthophosphate ($LaPO_4$) and lanthanum chloride (LaCl). All La compounds exhibit distinct spectral characteristics in the VNIR range, while only LaCl shows the diagnostic LREE features at 525, 580, 747, 804 and 872 nm (Fig. 10).

Discussion

This study demonstrates that each REE has diagnostic spectral signatures in the VNIR and SWIR ranges. Whereas some REO display only weak features in the VNIR range, REE minerals show diagnostic features in the VNIR range. The three strongest absorption peaks shared by the LREE minerals and the LREO around 747, 804 and 872 nm are probably related to Nd, while the three strongest absorption peaks shared by the HREE minerals and the HREO at around 656, 804 and 908 nm are probably related to Dy, Ho, Er and Yb. HREE and LREE can be distinguished by these VNIR features. However, it is important to note that these key features can be absent when REE are located in a different compound, as shown by the La and Pr examples.

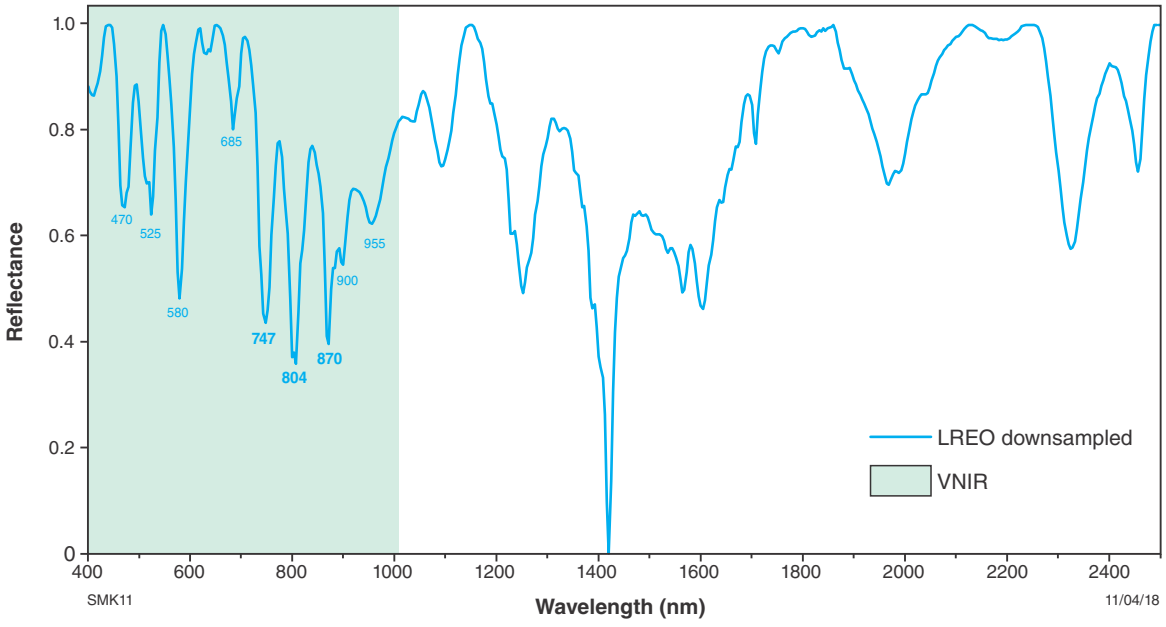

Figure 6. Spectra of light rare earth oxides (LREO) combined using the downsample technique; the three most characteristic features are in bold

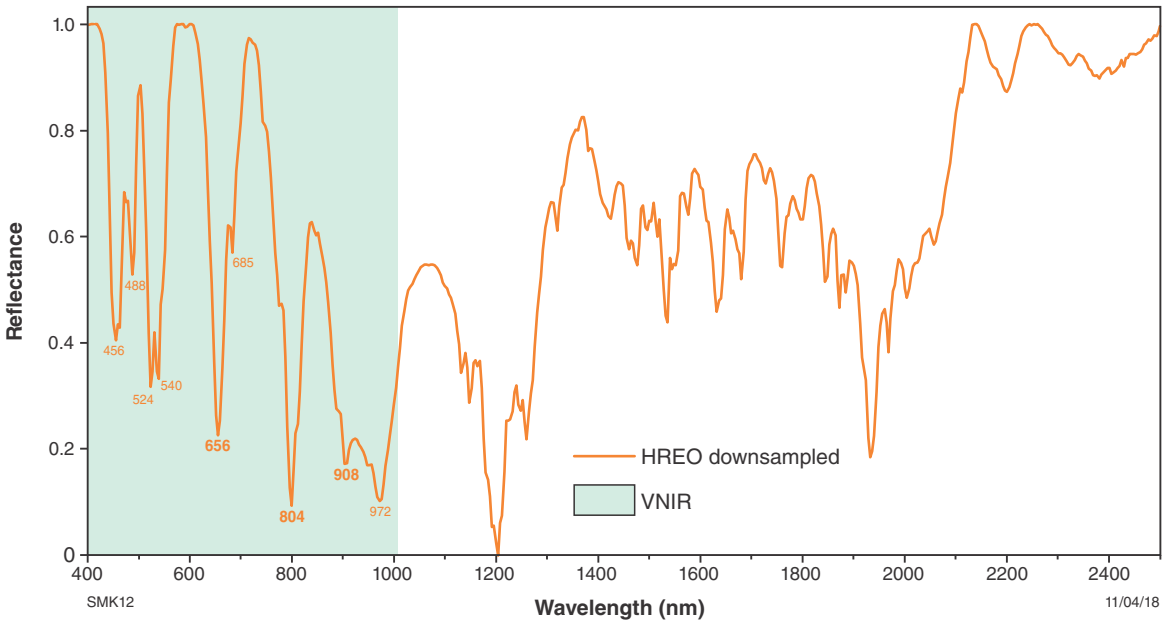

Figure 7. **Spectra of heavy rare earth oxides (HREO) combined using the downsample technique; the three most characteristic features are in bold**

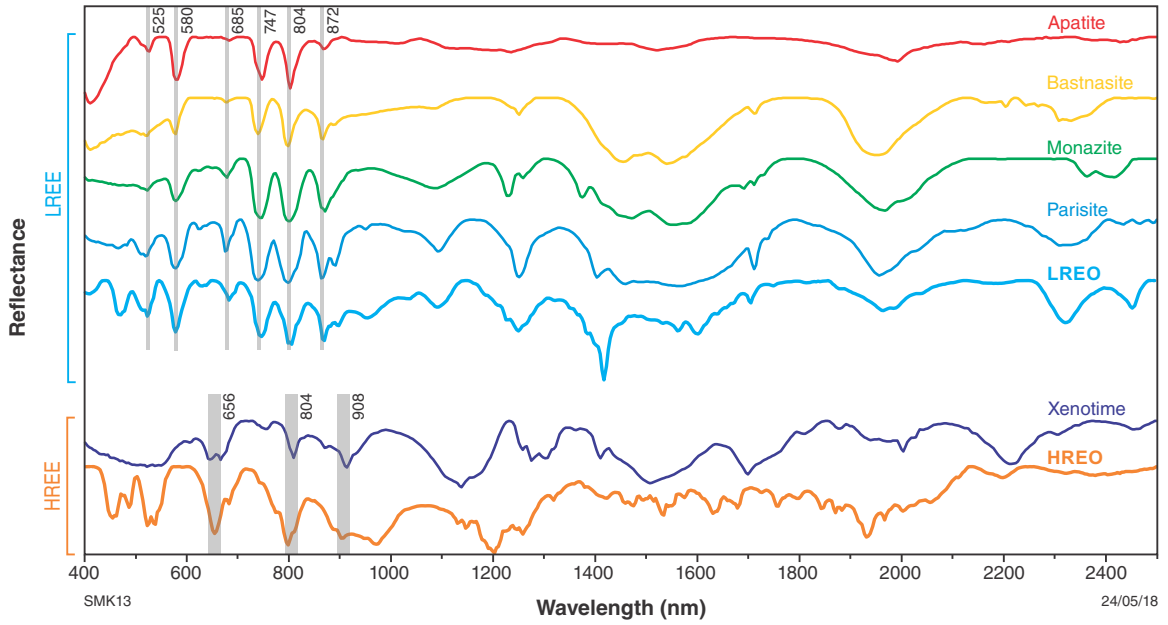

Figure 8. **Comparison of spectra from LREO, HREO and REE-bearing minerals. Monazite, apatite, bastnäsite and parisite are compared with LREO, and xenotime is compared HREO. Highlighted are the most characteristic features that correspond to the LREE and HREE signatures, respectively**

Table 1. Comparison of REE features of the minerals, monazite, apatite, bastnäsite, parisite and xenotime with downsampled LREO and HREO features

LREE	Absorption features in nanometers (nm)													
Monazite $(LREE)PO_4$					581		680	745	802	872				
Apatite $(REE, Ca)_5[(Si,P)O_4]_3X$					582			747	805	873				
Bastnäsite $LREE(CO_3)F$					578		680	742	800	868	892			
Parisite $Ca(LREE)_2(CO_3)_3F_2$					580		680	740	800	868	892			
LREO		470		525	580		685	747	804	872	900		955	
HREE														
Xenotime YPO_4						660			809			912		
HREO	457		488	525	540	656	685		804			908		972

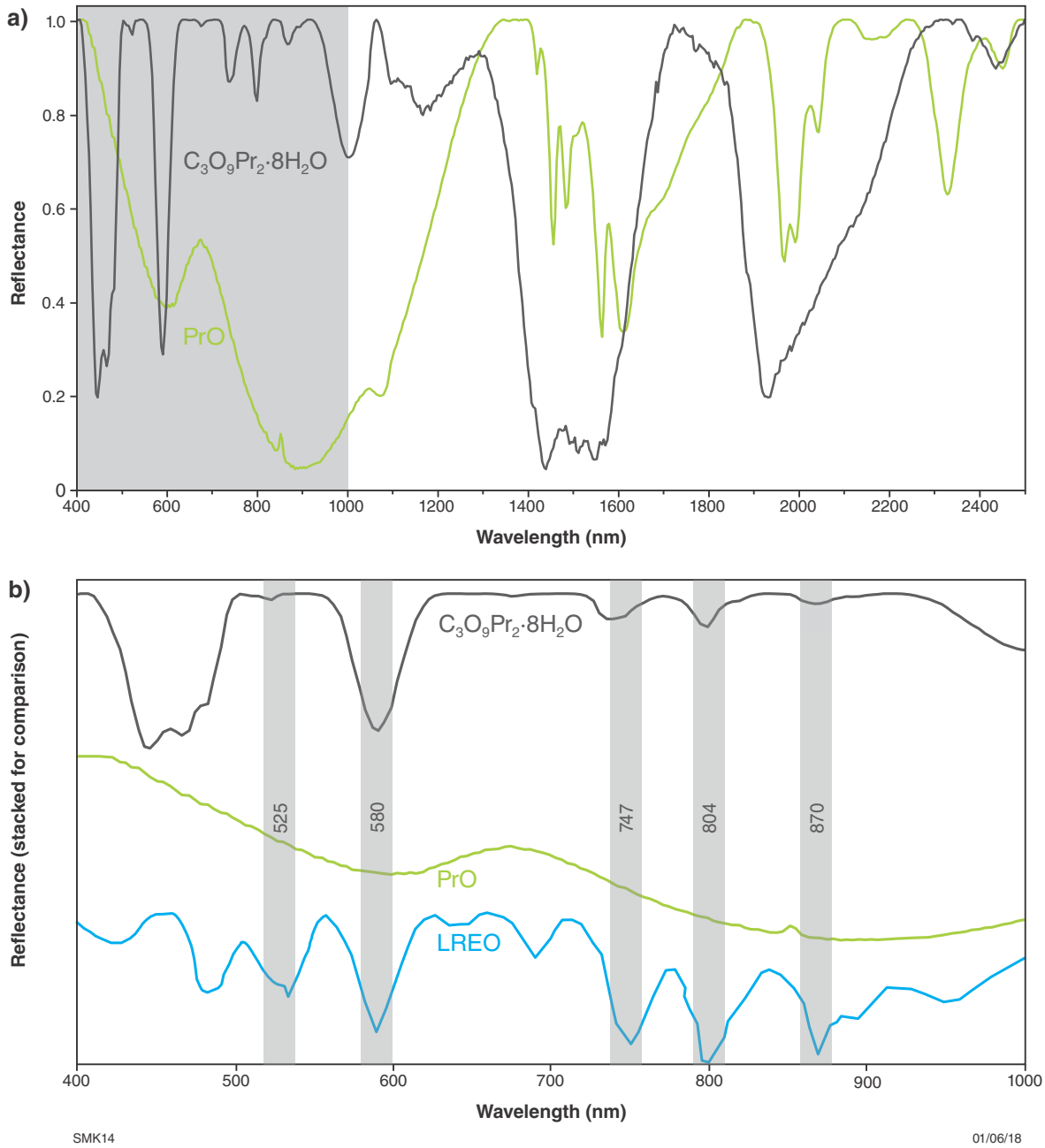

Figure 9. Comparison of two compound forms of the same element (Pr) and LREO in VNIR and SWIR ranges: a) praseodymium oxide (PrO) and Pr-carbonate-otcahydrate ($C_3O_9Pr_2{\cdot}8H_2O$) in VNIR and SWIR ranges; b) praseodymium oxide (PrO), Pr-carbonate-otcahydrate ($C_3O_9Pr_2{\cdot}8H_2O$) and LREO in VNIR range

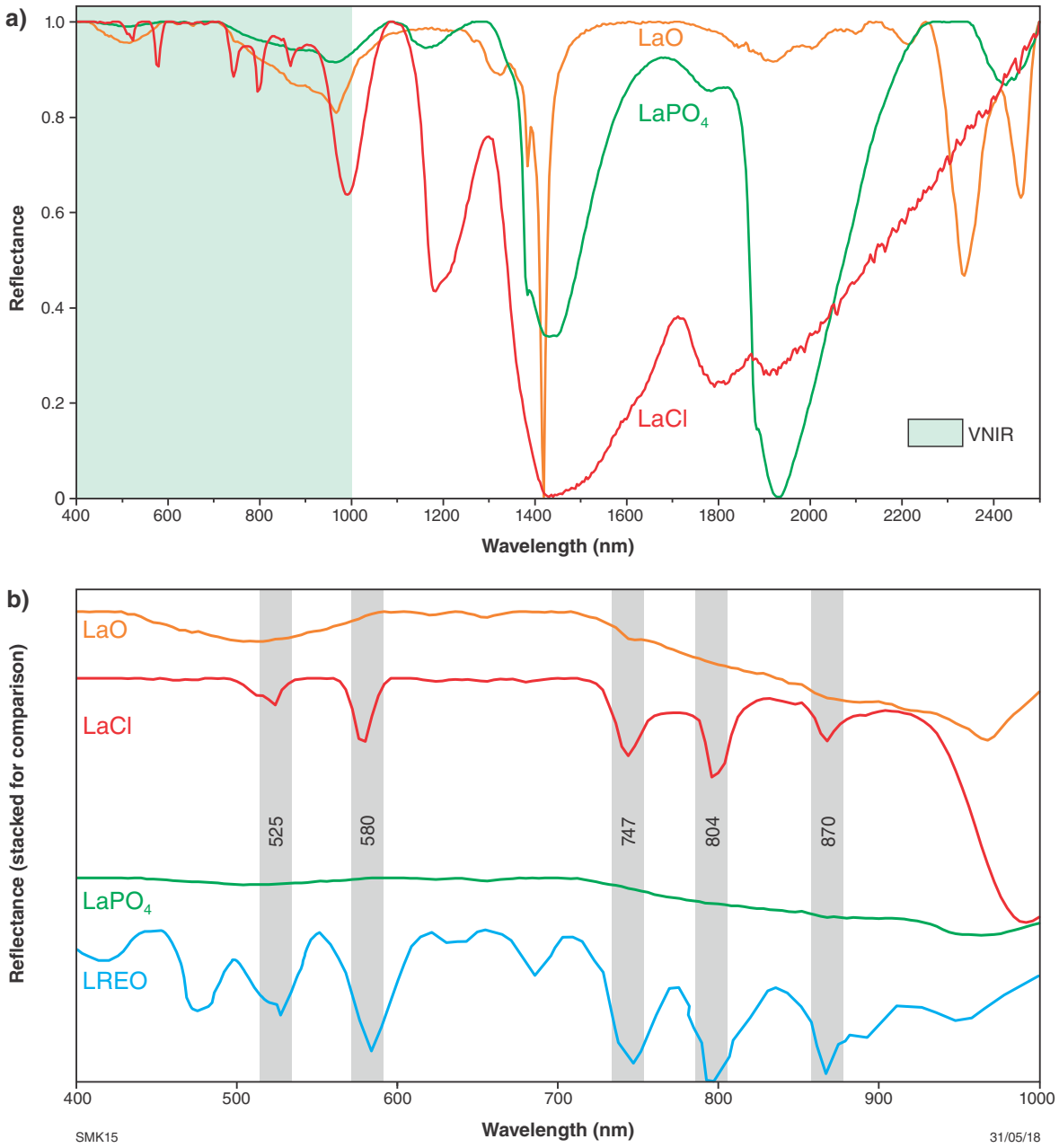

Figure 10. Comparison of three compound forms of the same element (La) and LREO in VNIR and SWIR ranges: a) lanthanum oxide (LaO), lanthanum orthophosphate ($LaPO_4$) and lanthanum chloride (LaCl) in VNIR and SWIR ranges; b) lanthanum oxide (LaO), lanthanum orthophosphate ($LaPO_4$), lanthanum chloride (LaCl) and LREO in VNIR range

Table 2. Compilation of the locations, coordinates, ages, ore minerals, alterations and references of REE deposits studied

Deposits	*Location*	*Coordinates Long./Lat.*	*Style*	*Age*	*Ore minerals*	*Alteration*	*References*
Brockman	17 km southeast of Halls Creek, east Kimberley	127.7820325 –18.319196	HREE & LREE Alkaline igneous rocks	Unknown	Gel-zircon Y-REE niobates Bastnäsite	Unknown	Taylor et al., 1995a,b Ramsden et al., 1993
Browns Range	160 km east of Halls Creek, east Kimberley	128.925085 –18.899857	HREE Hydrothermal veins	1646 ± 5.1 Ma	Xenotime Florencite	Clay rich alteration	Morin-Ka et al., 2016 Cook et al., 2013
Cummins Range	150 km south of Halls Creek, east Kimberley	127.1760141 –19.285821	LREE Laterite associated with carbonatite complexes	1009 ± 16 Ma	Monazite Apatite Bastnäsite Allanite Pyrochlore	Fenitization	Morin-Ka, 2018
Cundeelee	180 km east of Kalgoorlie, East Yilgarn	123.274402 –30.53577	LREE Carbonatite plug	Unknown	Unknown	Unknown	Lewis, 1990 Duncan, 1987
Gifford Creek	Northern Gascoyne	116.197215 –23.890331	LREE Ferro-carbonatite	1361 ± 10 Ma	Monazite Bastnäsite Pyrochlore Ferrocolumbite	Fenitization	Zi et al., 2017 Pirajno et al., 2014
John Galt	240 km south of Kununurra, east Kimberley	128.228945 –17.292781	HREE	1619 ± 8.8 Ma	Xenotime Florencite	Unknown	Morin-Ka, 2015 Reisgys, 1992
Mount Weld	300 km north of Kalgoorlie, East Yilgarn	122.5475227 –28.859949	LREE Laterite associated with carbonatite complexes	2021 ±13 Ma	Monazite Apatite Pyrochlore Churchite	Fenitization	Duncan et al., 1990

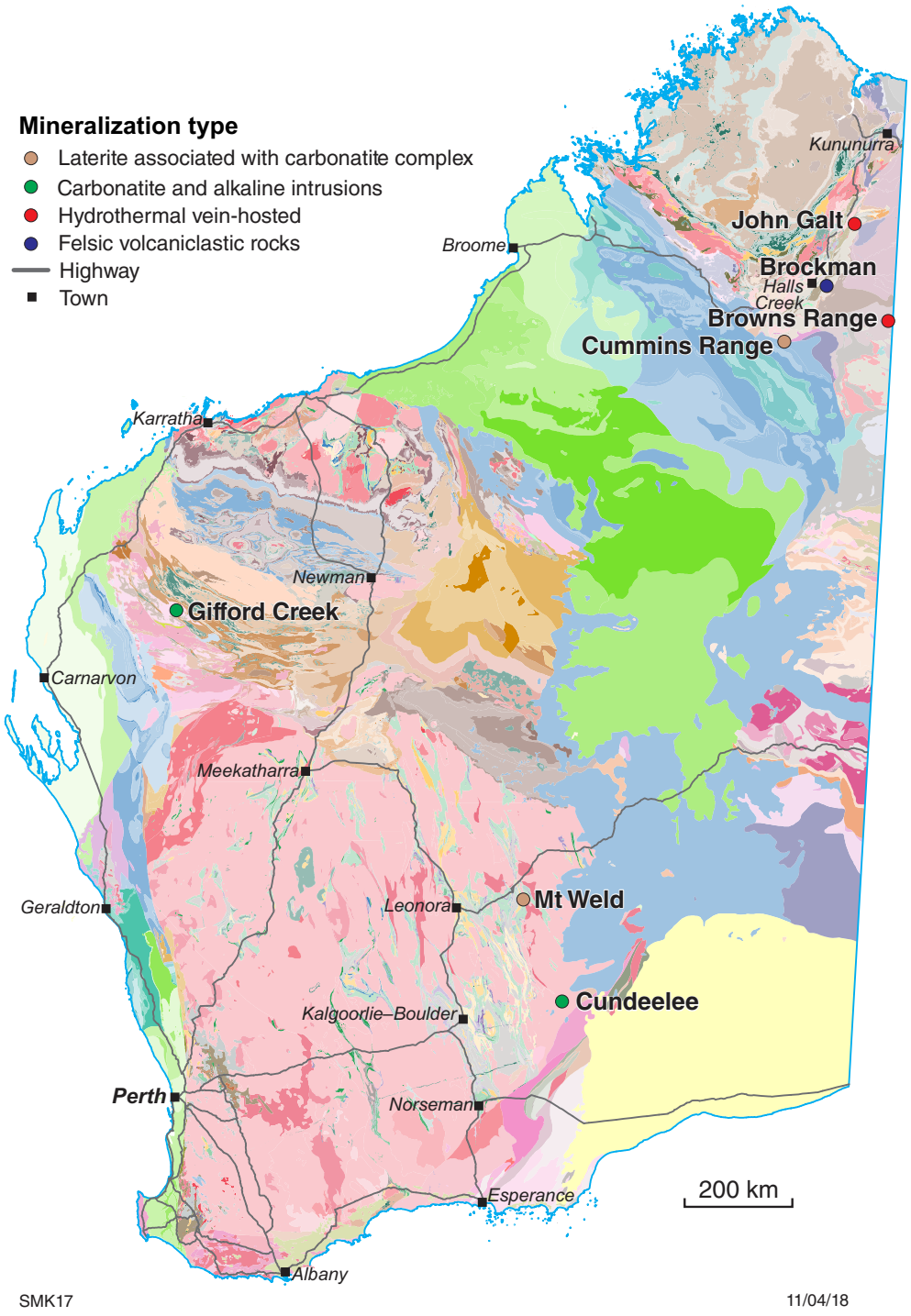

Figure 11. Map of Western Australia showing the location and mineralization types of REE deposits in this study

This can likely be explained by changes in the cation's specific coordination and asymmetry in the host crystal structure, as confirmed by the detailed work on this subject by Turner et al. (2014, 2016). However, the common ore minerals that were tested in Morin-Ka (2012) all display these diagnostic features, which may be explained by the presence of more than one REE in any ore mineral.

Rare earth elements

In this section, seven REE deposits and prospects in Western Australia hosted by carbonatite, alkaline igneous rocks, hydrothermal veins and laterite (Fig. 11; Table 2) were sampled with the aim of determining the spectral signature of their representative ores. From these occurrences, the Mount Weld and Brown Range deposits were chosen for detailed comparison on the basis that they are the best examples of LREE and HREE mineralization, respectively.

Methodology

Drillcore samples were scanned from the Mount Weld, Cummins Range (Morin-Ka, 2012) and Cundeelee drillholes, as well as selected hand specimens obtained from surface exposures at the Brockman, Browns Range, Gifford Creek, and John Galt deposits and prospects (Table 2). All samples were cleaned of foreign material attached to their surfaces (e.g. dust and particles) prior to scanning. The HyLogger was operated in continuous-scan mode, with spatial resolution of 8 mm and spectral resolution of 4 mm.

Spectra derived from the continuous scanning of samples were interrogated for the presence of diagnostic REE spectral features: 747, 804 and 872 nm features for LREE, and 656, 804 and 908 nm feature for HREE. A semi-automatic method was applied to search for these features, using scalars based on the polynomial fitted (PFIT) method. The PFIT method targets a specific absorption feature within a determined wavelength range and modulates its shape to extract the spectra that best fit.

Results

REE are considered to have been confidently detected when three diagnostic spectral features are identified in one sample. This study identified REE in four of the deposits: Browns Range, Cummins Range, Cundeelee and Mount Weld (Table 3). Of these four deposits, three display LREE signatures while Browns Range displays the only HREE signature (Table 3).

The samples from the Cundeelee prospect are dark; hence, they display only minor reflection of light and a low signal-to-noise ratio. REE detection was less accurate in these samples.

Mount Weld LREE deposit

The Mount Weld carbonatite is located near Laverton in the Eastern Goldfields Superterrane of the Yilgarn Craton (Fig. 11). It intrudes an Archean volcano-sedimentary sequence and is overlain by a thick lateritic regolith that is covered by lacustrine and alluvial sediments (Duncan and Willett, 1990). Mineralization is the result of enrichment through weathering of the carbonatite plug. The greatest enrichments of LREE (up to 24% LREO), are located in the lateritic profile. CH15 diamond drillcore provided by Lynas Corporation intersects the mineralized zone and penetrates underlying fresh carbonatite. Geochemical data include data obtained by DMIRS for the fresh carbonatite, and data provided by Lynas Corporation for the lateritic profile.

Although HREE are not identified, abundant LREE signatures are detected for the core, correlating with the distribution of LREE independently determined by geochemical analysis (Fig. 12). LREE signatures are more frequent and have higher amplitudes in the fresh carbonatite compared with the regolith signatures (Fig. 12). This was a surprising outcome considering that REO concentrations determined by geochemical analysis average 7.89% in the regolith which is 8.7 times higher compared with the 0.9% average in the fresh rocks. This observation is likely due to the scattering of light by the broken core in the regolith. In addition, the ferruginous composition of the core in these zones produces broad Fe^{3+} absorption in the VNIR range. Consequently, the reflected spectra do not have clearly defined spectral features, which translate to subdued REE signatures.

Browns Range HREE deposit

The Browns Range dome spans the border between Western Australia and the Northern Territory, located between the east Kimberley and northern Tanami deserts (Fig. 11). Bedrock in the area includes metamorphosed Archean metasedimentary rocks and Paleoproterozoic arkoses that record multiple deformation events (Cook et al., 2013). The deposit comprises mainly HREE minerals (i.e. xenotime), with minor LREE minerals (i.e. florencite).

Seven samples were collected from outcrop in several prospects in the Browns Range dome and were scanned with the HyLogger. None of the samples displayed LREE signatures. Only sample GSWA 206218 displays all the diagnostic HREE spectral features, indicating the likely presence of xenotime (i.e. similar to the signature determined for xenotime by Morin-Ka (2012; Fig. 13).

Discussion

The examination of samples of drillcore and hand specimens demonstrates that hyperspectral studies can identify and distinguish LREE and HREE using their key diagnostic spectral features. Furthermore, REE can be detected in fresh and weathered rocks despite the more subdued spectral expression in regolith materials due to the presence of ferric iron, which have a broad response in the VNIR range.

Table 3. Compilation of the results of REE detection for the samples studied

Deposit/Prospect	*Results*
Hand samples	
Brockman HREE-bearing deposit	Outcrop GSWA 206204B and GSWA 206205 samples show only very weak REE signatures that may refer to background noise
Browns Range HREE mineralization	Outcrop GSWA 206218 sample from Wolverine prospect outcrop shows HREE signatures
Gifford Creek LREE mineralization	No REE signatures found
John Galt HREE mineralization	No REE signatures found
Drillcores	
Cummins Range LREE mineralization	DD84CDD1 and DD84CDD2 drillholes show 697 and 779 LREE signatures respectively
Cundeelee Carbonatite plug, mineralized?	CDD001 shows three HREE locations and 14 LREE signatures that may refer to background noise due to the low reflection of the core
Mount Weld LREE mineralization	CH15 shows 228 LREE signatures found all along the drillcore

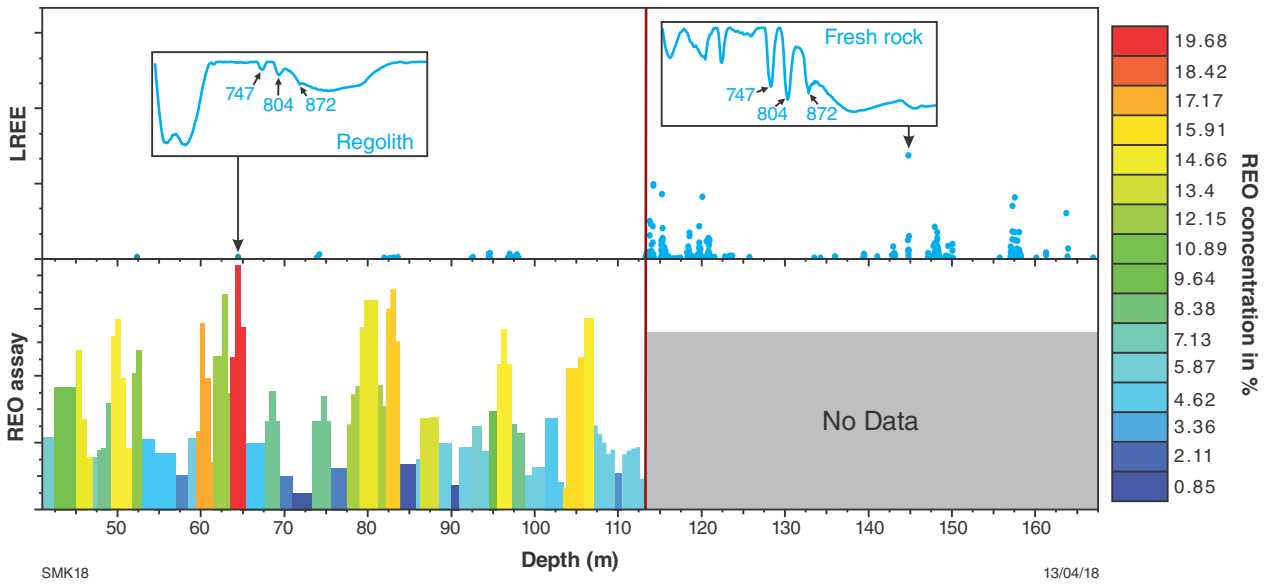

Figure 12. Mount Weld CH15 downhole log of REO concentration in percent compared with the response for detection of REE; no assays were collected below 110 m; the red line defines the transition from regolith (0–110 m) to fresh rock (below 110 m)

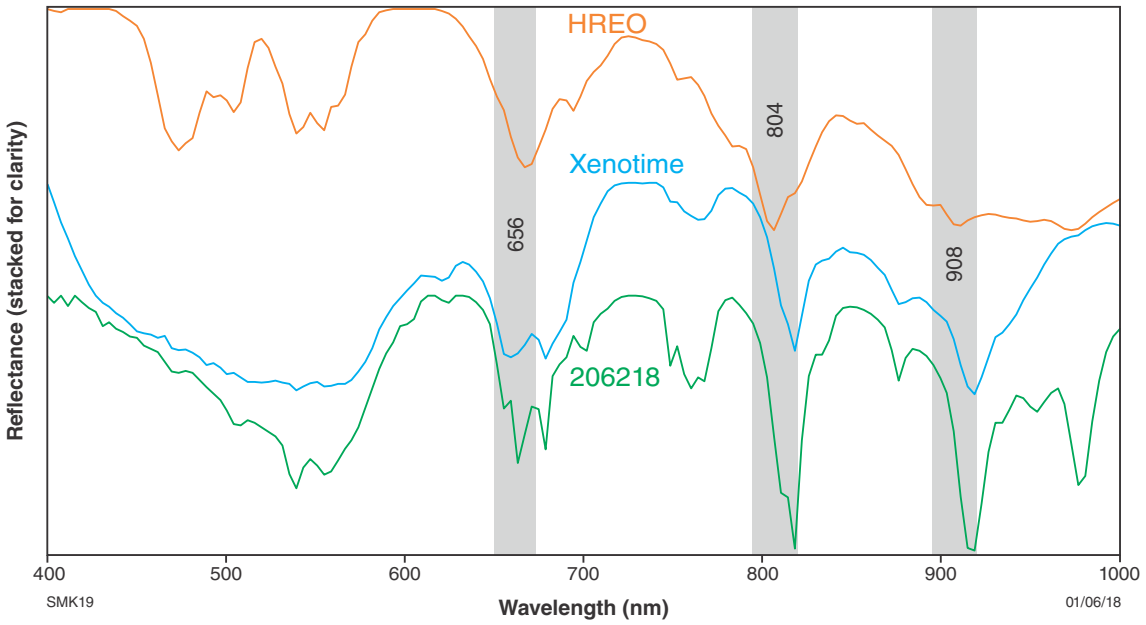

Figure 13. Comparison of HREO, xenotime and GSWA sample 206218 spectra in VNIR range

Automated detection of rare earth elements

LREE features at 747, 804 and 872 nm and HREE features at 656, 804 and 908 nm are effective for detecting REE in spectral data. The development of an automated search using these diagnostic features enables the rapid identification of REE and allows LREE and HREE to be differentiated.

Scalars offer a quick and accurate method for automatically identifying features in scanned samples. They are created using the TSG software to provide the automatic recognition of all three diagnostic features for REE in a spectrum. Scalars are created for both LREE and HREE using the PFIT method, which targets the geometry of spectral features within a specified wavelength range. The scalar identifies the presence of the first feature. Using the logical function '*AND*', the scalar then tests whether the second feature is present, followed by testing for the coexistence of the third feature. If any one of the features is missing, the scalar will produce no result. Each of these diagnostic features is determined by two factors: its wavelength and shape (Fig. 14). To locate a feature, the PFIT method will search an area within the fitting interval that corresponds to where the feature should be. The search will then focus on the narrow interval to find an apex that corresponds to the wavelength of the searched feature (Fig. 14). The minimum and maximum search range allows for a shift in the feature's position either side of the predicted wavelength. A 5th-order polynomial provides the best possible fit in most cases. A minimal depth value of 0.01 is applied to the filter searching the features to prevent identifying noise as a signal. The LREE scalar is expressed in Figure 15, whereas the HREE scalar is shown in Figure 16. A third scalar is provided to test for the presence of any REE (Fig. 17) by combining the scalars for LREE (Fig. 15) and HREE (Fig. 16) using the logical function '*OR*'. These scalars need to be loaded into TSG using the BATCH method within the TSG scalar creation tool (Fig. 18a). The scripts in Figures 15, 16 or 17 should be copied into the 'edit script' window (Fig. 18b) In addition, if the dataset has masks attached, these masks can be selected in the 'BATCH method' window (Fig. 18).

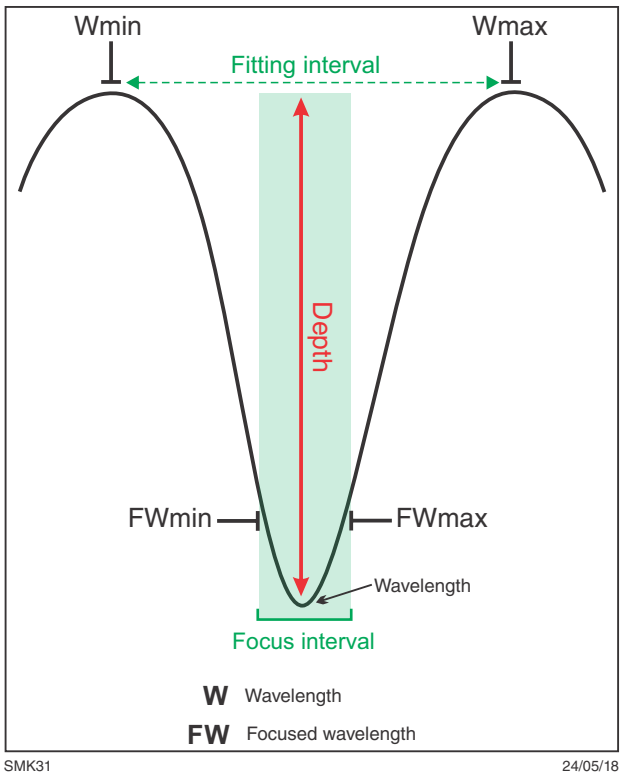

Figure 14. Diagram illustrating how a feature is fitted using the PFIT method

Commands = 1 Name = LREE,5	Number of command Name of scalar and number of parameter
P1 = Pfit, layer=Reflectance, wunits=nm, wmin=710, wmax=780, fwmin=737, fwmax=757, maxrmse=0, minval=0.01, minarea=0, bktype=1, bksub=0, order=5, product=1 P2 = Pfit, layer=Reflectance, wunits=nm, wmin=770, wmax=840, fwmin=790, fwmax=817, maxrmse=0, minval=0.01, minarea=0, bktype=1, bksub=0, order=5, product=1 P3 = Pfit, layer=Reflectance, wunits=nm, wmin=850, wmax=890, fwmin=860, fwmax=880, maxrmse=0, minval=0.01, minarea=0, bktype=1, bksub=0, order=5, product=1	LREE features search criteria
P4 = expr, arithop=11, param1=p1, param2=p2	Logical operation (AND) on the criteria
Return = expr, arithop=11, param1=p3, param2=p4	Final logical operation (AND) on the criteria

SMK22 24/05/18

Figure 15. The Spectral Geologist (TSG) scalar command set for LREE detection

Commands = 1 Name = HREE,5	Number of command Name of scalar and number of parameter
P1 = Pfit, layer=Reflectance, wunits=nm, wmin=615, wmax=680, fwmin=646, fwmax=666, maxrmse=0, minval=0.01, minarea=0, bktype=1, bksub=0, order=5, product=1 P2 = Pfit, layer=Reflectance, wunits=nm, wmin=775, wmax=835, fwmin=790, fwmax=817, maxrmse=0, minval=0.01, minarea=0, bktype=1, bksub=0, order=5, product=1 P3 = Pfit, layer=Reflectance, wunits=nm, wmin=891, wmax=930, fwmin=898, fwmax=918, maxrmse=0, minval=0.01, minarea=0, bktype=1, bksub=0, order=5, product=1	HREE features search criteria
P4 = expr, arithop=11, param1=p1, param2=p2	Logical operation (AND) on the criteria
Return = expr, arithop=11, param1=p3, param2=p4	Final logical operation (AND) on the criteria

SMK23 24/05/18

Figure 16. The Spectral Geologist (TSG) scalar command set for HREE detection

Commands = 1 Name = REE,11	Number of command Name of scalar and number of parameter
P1 = Pfit, layer=Reflectance, wunits=nm, wmin=710, wmax=780, fwmin=737, fwmax=757, maxrmse=0, minval=0.01, minarea=0, bktype=1, bksub=0, order=5, product=1 P2 = Pfit, layer=Reflectance, wunits=nm, wmin=770, wmax=840, fwmin=790, fwmax=817, maxrmse=0, minval=0.01, minarea=0, bktype=1, bksub=0, order=5, product=1 P3 = Pfit, layer=Reflectance, wunits=nm, wmin=850, wmax=890, fwmin=860, fwmax=880, maxrmse=0, minval=0.01, minarea=0, bktype=1, bksub=0, order=5, product=1	LREE features search criteria
P4 = Pfit, layer=Reflectance, wunits=nm, wmin=615, wmax=680, fwmin=646, fwmax=666, maxrmse=0, minval=0.01, minarea=0, bktype=1, bksub=0, order=5, product=1 P5 = Pfit, layer=Reflectance, wunits=nm, wmin=775, wmax=835, fwmin=790, fwmax=817, maxrmse=0, minval=0.01, minarea=0, bktype=1, bksub=0, order=5, product=1 P6 = Pfit, layer=Reflectance, wunits=nm, wmin=891, wmax=930, fwmin=898, fwmax=918, maxrmse=0, minval=0.01, minarea=0, bktype=1, bksub=0, order=5, product=1	HREE features search criteria
P7 = expr, arithop=11, param1=p1, param2=p2 P8 = expr, arithop=11, param1=p3, param2=p7 P9 = expr, arithop=11, param1=p4, param2=p5 P10 = expr, arithop=11, param1=p6, param2=p9	Logical operation (AND) on the criteria
Return = expr, arithop=12, param1=p8, param2=p10, nullhandling=3	Final logical test (OR)

SMK24 24/05/18

Figure 17. The Spectral Geologist (TSG) scalar command set for REE detection (either LREE or HREE)

a) BATCH method

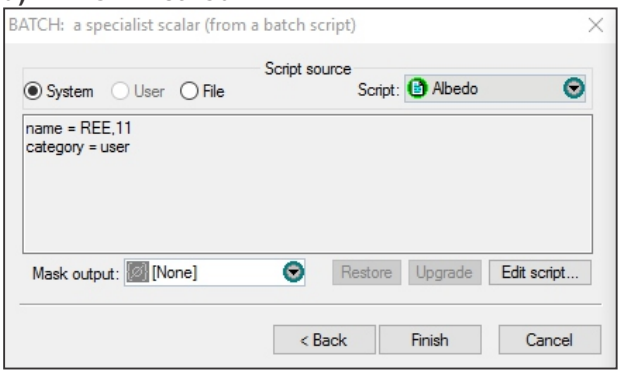

b) Edit script window

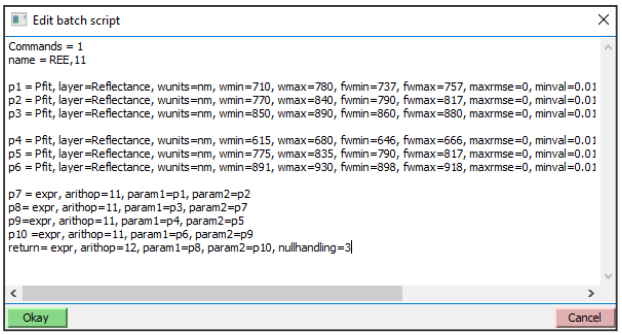

Figure 18. TSG scalar creation tool: a) BATCH method window: select 'Mask output' if applicable then click 'Edit script…'; b) edit script window: paste code from LREE, HREE or HREE scalars provided in Figures 15, 16 and 17 (see text for script details)

Conclusions

Sample preparation is critical for the accurate detection of fine-grained, disseminated REE-bearing minerals in unprocessed hand specimen, drillcore, powder and any other sample type. The samples should be free of dust and any contaminant on their surface.

Each REO exhibits unique, repeatable, consistent, strong and sharp absorption features in the VNIR and SWIR ranges — but returns no detectable features in the TIR range — and some absorption features are common to more than one element.

Contrary to expectation, REE phosphates, carbonates and chlorides standards returned VNIR absorption features different from those of their corresponding oxides. This phenomenon is likely due to changes in the crystal structure and specific cation's coordination. However, minerals, drillcores and samples studies always showed consistent REE signatures.

It is difficult to give an exact detection limit for REE without conducting further work to quantify the signature of known concentrations. Combining assay results with the scalars could be used to better define a limit. In any case, it would be specific to the geological and mineralogical setting. Although each REE has a unique spectral signature, the ratio of the contribution made by each element is not quantifiable because not every element responds equally in the VNIR range.

Iron oxide-rich material interferes with REE spectral signatures because their signatures overlap in the VNIR range. Accordingly, low REE concentrations are unlikely to be detected in iron-rich rocks.

Combined spectra for LREO and HREO were created to mimic the potential signatures of naturally occurring LREE and HREE minerals. The three most prominent features from each combined spectrum were selected to create diagnostic algorithms or 'scalars' that can be used to automatically identify the presence of REE and distinguish between LREE and HREE. These features occur at 747, 804 and 872 nm for LREE, and at 656, 804 and 908 nm for HREE. The expected diagnostic LREE or HREE signatures are consistently detected and distinguished using the scalars. However, the signatures are strongly influenced by absorption features of REE that have low concentrations in the principal REE minerals (e.g. Nd in LREE minerals; Dy, Ho, Er and Yb in HREE minerals), but the threshold below which they are not manifested is not yet known. Additionally, the LREE and HREE scalars show strong correlation with independently derived data (i.e. geochemistry and mineral petrological identification).

In conclusion, reflectance spectroscopy shows promise as an exploration tool for rapid, non-destructive detection and broad characterization of REE mineralization in powders, rock chips, drillcore, and outcrop.

Acknowledgements

The author would like to thank Dr John Huntington for providing constructive suggestions in regard to the treatment of the collected spectral data. Huntington Hyperspectral Pty Ltd, and the CSIRO Minerals Down Under Flagship and Earth Science and Resource Engineering are thanked for the provision of mineral standards.

The author would also like to acknowledge Northern Minerals Limited and Lynas Corporation for providing access to their drillcores and associated geochemical data in addition to their assistance in understanding their respective mineralized occurrences.

References

Adams, JW 1965, The visible region absorption spectra of rare-earth minerals: The American Mineralogist, v. 50, March–April, p. 356–366.

Christie, T, Brathwaite, B and Tulloch, A 1998, Mineral commodities report 17 — rare earths and related elements: New Zealand Institute of Geological and Nuclear Sciences Limited, 13p. (unpublished).

Clark, RN 1999, Spectroscopy of rocks and minerals, and principles of spectroscopy, *in* Manual of remote sensing (Volume 3: remote sensing for the earth sciences (3rd) edition) *edited by* AN Rencz and RA Ryerson: Wiley and Sons, Inc., New York, USA, p. 3–58.

Cook, N, Ciobanu, C, O'Rielly, D, Wilson, R, Das, K and Wade, B 2013, Mineral chemistry of rare earth element (REE) mineralization, Browns Ranges, Western Australia: Lithos, v. 172, p. 192–213.

Dill, HG 2010, The "chessboard" classification scheme of mineral deposits: Mineralogy and geology from aluminum to zirconium: Earth-Science Reviews, v. 100, no. 1, p. 1–420.

Duncan, RK 1987, Final report on exploration E.L. 28/131 Ponton Creek; Union Oil Development Corporation: Geological Survey of Western Australia, Statutory mineral exploration report, A21981, 25p.

Duncan, RK and Willett, GC 1990, Mount Weld Carbonatite: Monograph Series – Australasian Institute of Mining and Metallurgy, v. 14, p. 591–597.

Görller-Walrand, C and Binnemans, K 1998, Chapter 167 Spectral intensities of f-f transitions, *edited by* AG Karl: Elsevier, Handbook on the Physics and Chemistry of Rare Earths, v. 25, p. 101–264.

Hancock, EA and Huntington, JF 2010, The GSWA HyLogger: rapid spectral analysis and its application in detecting mineralization, *in* GSWA 2010 extended abstracts: promoting the prospectivity of Western Australia: Geological Survey of Western Australia, Record 2010/2, p. 10–13.

Hancock, E, Green, A, Huntington, J, Schodlok, M and Whitbourn, L 2013, HyLogger-3: Implications of adding thermal-infrared sensing: Geological Survey of Western Australia, Record 2013/3.

Lewis, JD 1990, Chapter 5 – Diatremes, *in* Geology and Mineral Resources of Western Australia: Geological Survey of Western Australia, Memoir 3, p. 589.

Morin-Ka, S 2012, Hyperspectral characterization of rare earth minerals: Geological Survey of Western Australia, Record 2012/12, 50p.

Morin-Ka, S, Hancock, EA and Beardsmore, TJ 2014, Exploring for rare earth elements using reflectance spectroscopy (Abstract No 110), *in* Abstracts: Geological Society of Australia; Australian Earth Sciences Convention (AESC), Sustainable Australia, Newcastle, NSW, 7 July 2014.

Morin-Ka, S and Beardsmore,TJB 2015, Overview of the REE mineralization in the East Kimberley – West Tanami region, *in* GSWA Kimberley workshop 2014: extended abstracts *compiled by* DW Maidment: Geological Survey of Western Australia, Record 2015/6, p. 50–51.

Morin-Ka, S, Beardsmore, T, Hancock, EA, Rasmussen, B, Dunkley, DJ, Zi, J, Muhling, JR, Wilson, R and Chapman, J 2016, Alteration and age of the Browns Range heavy rare earth deposits, *in* GSWA 2016 extended abstracts: promoting the prospectivity of Western Australia: Geological Survey of Western Australia, Record 2016/2, p. 21–25.

Morin-Ka, S 2018, Cummins Range carbonatite (P_-_cu-xax-r): Geological Survey of Western Australia, WA Geology Online, Explanatory Notes extract, viewed 19 April 2018, <www.dmp.wa.gov.au/ens>.

Pirajno, F, Gonzalez-Alvarez, I, Chen, W, Kyser, KT, Simonetti, A, Leduc, E and LeGras, M 2014, The Gifford Creek Ferrocarbonatite Complex, Gascoyne Province, Western Australia: Associated fenitic alteration and a putative link with the ~1075 Ma Warakurna LIP: Lithos, v. 202–203, p. 100–119.

Ramsden, AR, French, DH and Chalmers, DI 1993, Volcanic-hosted rare-metals deposit at Brockman, Western Australia; mineralogy and geochemistry of the Niobium Tuff: Mineralium Deposita, v. 28, no. 1, p. 1–12.

Reisgys, L 1992, Annual report May 1991 – May 1992 Mining Lease 80/40 East Kimberley, Western Australia; REO Corporation Limited: Geological Survey of Western Australia, Statutory mineral exploration report, A36426.

Taylor, WR, Page, RW, Esslemont, G, Rock, NMS and Chalmers, DI 1995a, Geology of the volcanic-hosted Brockman rare-metals deposit, Halls Creek mobile zone, Northwest Australia; 1, Volcanic environment, geochronology and petrography of the Brockman Volcanics: Mineralogy and Petrology, v. 52, no. 3-4, p. 209–230.

Taylor, WR, Esslemont, G and Sun, SS 1995b, Geology of the volcanic-hosted Brockman rare-metals deposit, Halls Creek mobile zone, Northwest Australia; 2, Geochemistry and petrogenesis of the Brockman Volcanics: Mineralogy and Petrology, v. 52, no. 3–4, p. 231–255.

Turner, DJ, Rivard, B and Groat, LA 2014, Visible and short-wave infrared reflectance spectroscopy of REE fluorocarbonates: American Mineralogist, v. 99, no. 7, p. 1335–1346.

Turner, DJ, Rivard, B and Groat, LA 2016, Visible and short-wave infrared reflectance spectroscopy of REE phosphate minerals: American Mineralogist, v. 101, no. 9–10, p. 2264.

United States Geological Survey (compiler) 2018, Rare earths: U.S. Geological Survey, Mineral commodity summaries 2018, p. 132–133.

Verplanck, PL and Van Gosen, BS 2011, Carbonatite and alkaline intrusion related REE deposits — A deposit model: U.S. Geological Survey Open-File Report 2011–1256, 6p.

Zi, JW, Gregory, C, Rasmussen, B, Sheppard, S and Muhling, JR 2017, Using monazite geochronology to test the plume model for carbonatites: The example of Gifford Creek Carbonatite Complex, Australia: Chemical Geology, v. 463, p. 50–60.

This study demonstrates that reflectance spectroscopy may be a viable exploration tool for rapid, non-destructive detection and broad characterization of rare earth element (REE) mineralization. Common REE-bearing mineral species are generally preferentially enriched in mixtures of either light or heavy REE. Spectroscopic analysis of Western Australian REE-bearing minerals in the visible to near infrared (VNIR) wavelength range reveals that the spectra for all light REE-enriched minerals share several absorption features, and those for all heavy REE-enriched minerals share several distinctively different features.
A comparison of natural mineral reflectance spectra with those for oxides of the 15 rare earth elements confirms that the prominent absorption features are produced by particular light or heavy REE. Such elements will likely always be present in natural REE-bearing minerals; hence, are valid proxies for general light or heavy REE enrichment. Spectral algorithms have therefore been created to automatically identify the presence of light or heavy REE in any VNIR spectrum.

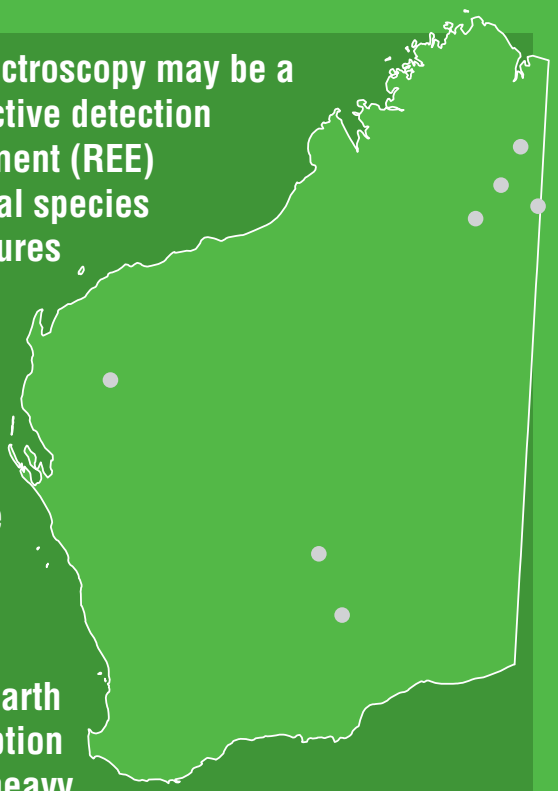

Further details of geological products and maps produced by the Geological Survey of Western Australia are available from:

Information Centre
Department of Mines, Industry Regulation and Safety
100 Plain Street
EAST PERTH WA 6004
Phone: (08) 9222 3459 Fax: (08) 9222 3444

www.dmp.wa.gov.au/GSWApublications

MORIN-KA

DETECTION AND IDENTIFICATION OF RARE EARTH ELEMENTS USING HYPERSPECTRAL TECHNIQUES

REPORT 187